NREL/TP-451-21586 • UC Category: 1263 • DE96013077

Device Physics of Thin-Film Polycrystalline Cells and Modules

Annual Subcontract Report, 6 December 1994 - 5 December 1995

J.R. Sites
Department of Physics
Colorado State University
Fort Collins, Colorado

NREL technical monitor: B. von Roedern

National Renewable Energy Laboratory
1617 Cole Boulevard
Golden, Colorado 80401-3393
A national laboratory of
the U.S. Department of Energy
Managed by Midwest Research Institute
for the U.S. Department of Energy
under Contract No. DE-AC36-83CH10093

Prepared under Subcontract No. XAX-4-14000-01

August 1996

NOTICE

Available to DOE and DOE contractors from:
Office of Scientific and Technical Information (OSTI)
P.O. Box 62
Oak Ridge, TN 37831
Prices available by calling (423) 576-8401

Available to the public from:
National Technical Information Service (NTIS)
U.S. Department of Commerce
5285 Port Royal Road
Springfield, VA 22161
(703) 487-4650

SUMMARY

A number of projects have been carried out at both the cell and the module level during the past year:

(1) The effects of CdS thickness has been investigated in collaboration with six CdTe cell–fabrication laboratories. Photocurrent due to photons with energy greater than the CdS bandgap varies with thickness over a practical range from 1 to 5 mA/cm^2. There appears, however, to be a critical thickness, between 500 and 1000 Å depending on fabrication process, below which junction quality is degraded.

(2) An experimental and modeling project has shown that conduction band offsets less than about 0.3 eV have little effect on the performance of a $CuInSe_2$ (CIS) or CdTe cell under the traditional assumption that the absorber material accounts for most of the depletion region. There appears to be an exception, however, in some $CuInSe_2$ cells that have a significant thickness of n^-–CdS. In these cases the J–V curve is distorted and there can be a significant lack of light/dark superposition.

(3) Several other cell projects include the role of Ga distribution in $CuIn_{1-x}Ga_xSe_2$ (CIGS) cells, changes that occur in some cells over time, optical characterization of commonly–used CdTe substrates and front contacts, and comparative characterization of CIGS cells where identical absorbers were combined with variations in window fabrication.

(4) The primary module–characterization project was the successful use of chopping–frequency variation in a scanning beam to separate photocurrent and shunting problems affecting individual cells of an encapsulated module. This technique allows an expeditious evaluation of modules without having to access the individual cells.

(5) Other module projects included modifications in analysis required by the typical module–cell geometry, the practical effect of nonuniformities in light intensity or cell temperature, and the advantages and pitfalls of forward bias across a module during a light scan.

(6) Our lab has actively participated in both the CdTe and CIS teaming efforts that began in December 1994, and I have been part of the CIS–team leadership. The specific projects were the CdS thickness variations of CdTe cells and the different windows on common CIGS mentioned above.

TABLE OF CONTENTS

FIGURES

TABLE

INTRODUCTION

The objectives of the Colorado State program are (1) the separation and quantification of individual loss in specific thin–film solar cells, (2) the detailed characterization of small modules, and (3) the presentation of a viable model for the forward–current loss mechanism. Progress was made in each of these areas.

Five research students as well as Dr. Xiaoxiang Liu, who continued part–time as a postdoctoral researcher, were responsible for most of the experimental and analytical work. Ingrid Eisgruber did essentially all of the work on modules. She should complete her Ph.D. in early 1996 and will begin full–time work at the Materials Research Group. Jennifer Granata was responsible for systematic comparisons of both CdTe and CIS cells. Jon Sharp, Brendon Murphy, and Karl Schmidt worked on smaller projects focused on specific cells. Dr. Liu utilized the ADEPT software from Purdue University to model the possible effects of band offsets on solar–cell performance.

The Colorado State program continues to collaborate closely with a number of other laboratories. During the past year active collaborations have included the Institute of Energy Conversion, International Solar Electric Technology, Inc., the National Renewable Energy Laboratory, Solar Cells, Inc., Siemens Solar Industries, Solarex, Energy Photovoltaics, Inc., the University of South Florida, the University of Toledo, and the Colorado School of Mines.

CELL ANALYSIS

CdS Thickness

The thickness of a CdS window is particularly important for CdTe solar cells. The maximum photocurrent for the CdTe bandgap and a 100 mW/cm^2 global AM1.5 spectrum is just over 30 mA/cm^2. Nearly 25% of this photocurrent, or about 7.5 mA/m^2 comes from photons with energy above the CdS bandgap. For the lower–bandgap CIS cells, the maximum photocurrent is higher, and the potential loss from CdS absorption is closer to 15%. In both cases, however, it has been generally recognized that thinner CdS, or no CdS at all, would lead to higher photocurrents. Scattered results have indicated that while the photocurrent goes up, thinner CdS may result in overall less–efficient cells.

A systematic study was undertaken by seven members of the CdTe Device Team to document which parameters are affected by CdS thickness and whether the dependence is different for different fabrication techniques. CdTe cells were fabricated by NREL, University of Toledo (UT), Solar Cells, Inc. (SCI), University of South Florida (USF), Colorado School of Mines (CSM), and the Institute of Energy Conversion (IEC). In each case cells were made with a range of CdS thicknesses. All six fabrication labs used Corning 7059 superstrate, though UT used an LOF superstrate as well. Table I summarizes the deposition and thickness–measurement techniques.

Lab	NREL	UToledo	SCI	USF	CSM	IEC
CdS deposition technique	Chemical bath deposition	rf sputtering	CSS	CBD	CBD	Physical vapor deposition
CdS measurement technique	ellipso-metry (on glass side)	*in situ* optical absorption	deposition time	deposition time	surface profile	optical trans. of as-deposited CdS
CdTe deposition technique	Close-space sublimation	rf sputtering	CSS	CSS	electro-chemical deposition	PVD

Table I. Cells used to study CdS thickness effects.

Cell characterization was done by Jennifer Granata, who measured superstrate/TCO absorption, cell reflection, current–voltage, quantum efficiency, and capacitance. Figure 1 shows what happens to the photons for four otherwise–identical cells with different CdS thicknesses. The measured

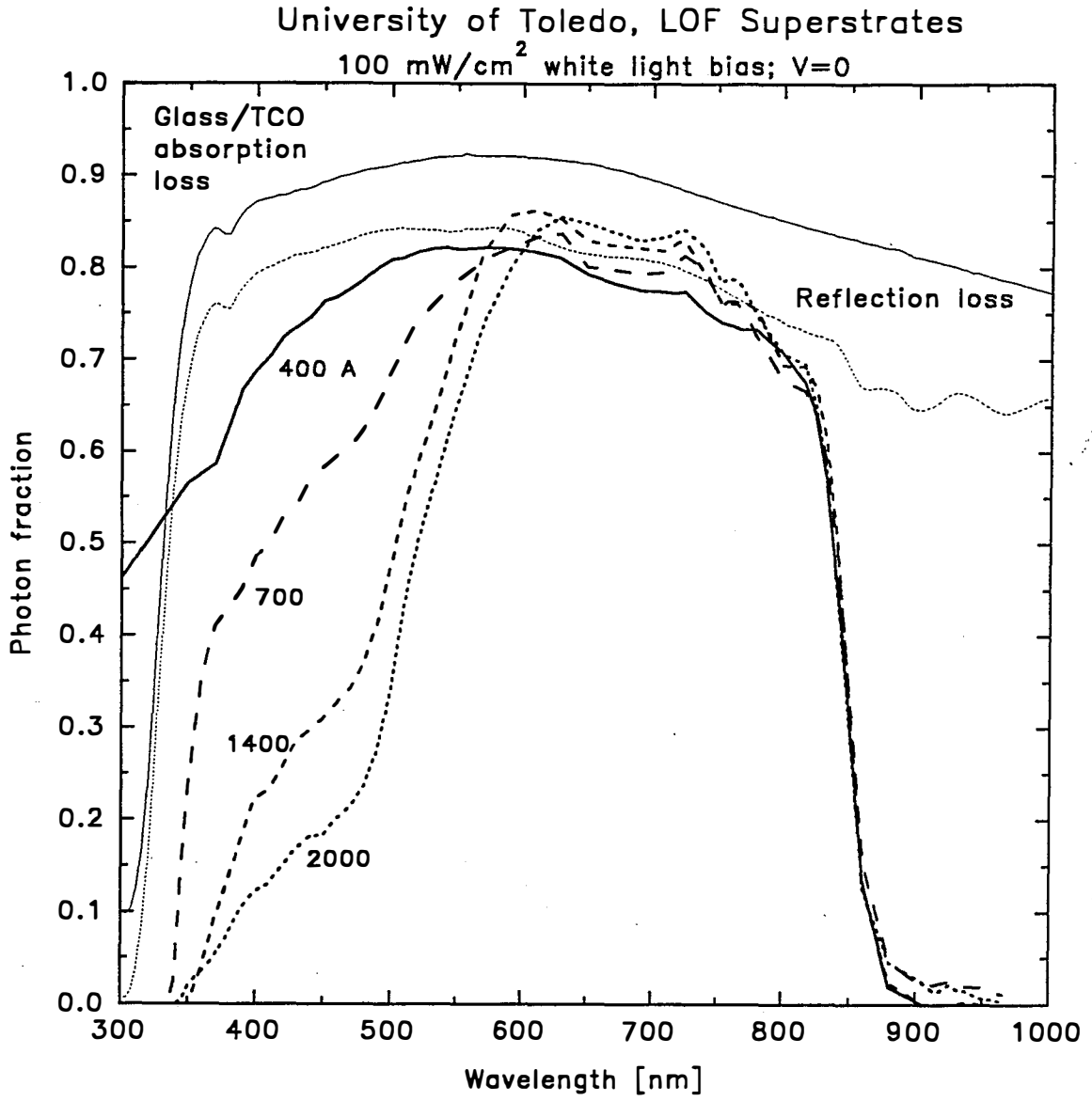

Figure 1. Quantum efficiency and optical losses for four University of Toledo cells with varying CdS thickness. Measurements made at Colorado State and NREL show good agreement.

glass/TCO–absorption and cell–reflection losses are indicated. These account for most of the mid–wavelength photon losses. At short wavelengths, however, there are major quantum efficiency differences. These can be used to calculate the photocurrent due to photons with wavelengths less

than 520 nm, which corresponds to the CdS bandgap. This contribution to the photocurrent is shown in Fig. 2 for all the cells measured. As expected, it decreases smoothly with increasing CdS thickness, and can be reasonably approximated by an exponential curve. Also shown in Fig. 2 is an earlier cell from Photon Energy (PE) [1], which has the largest short–wavelength collection seen in

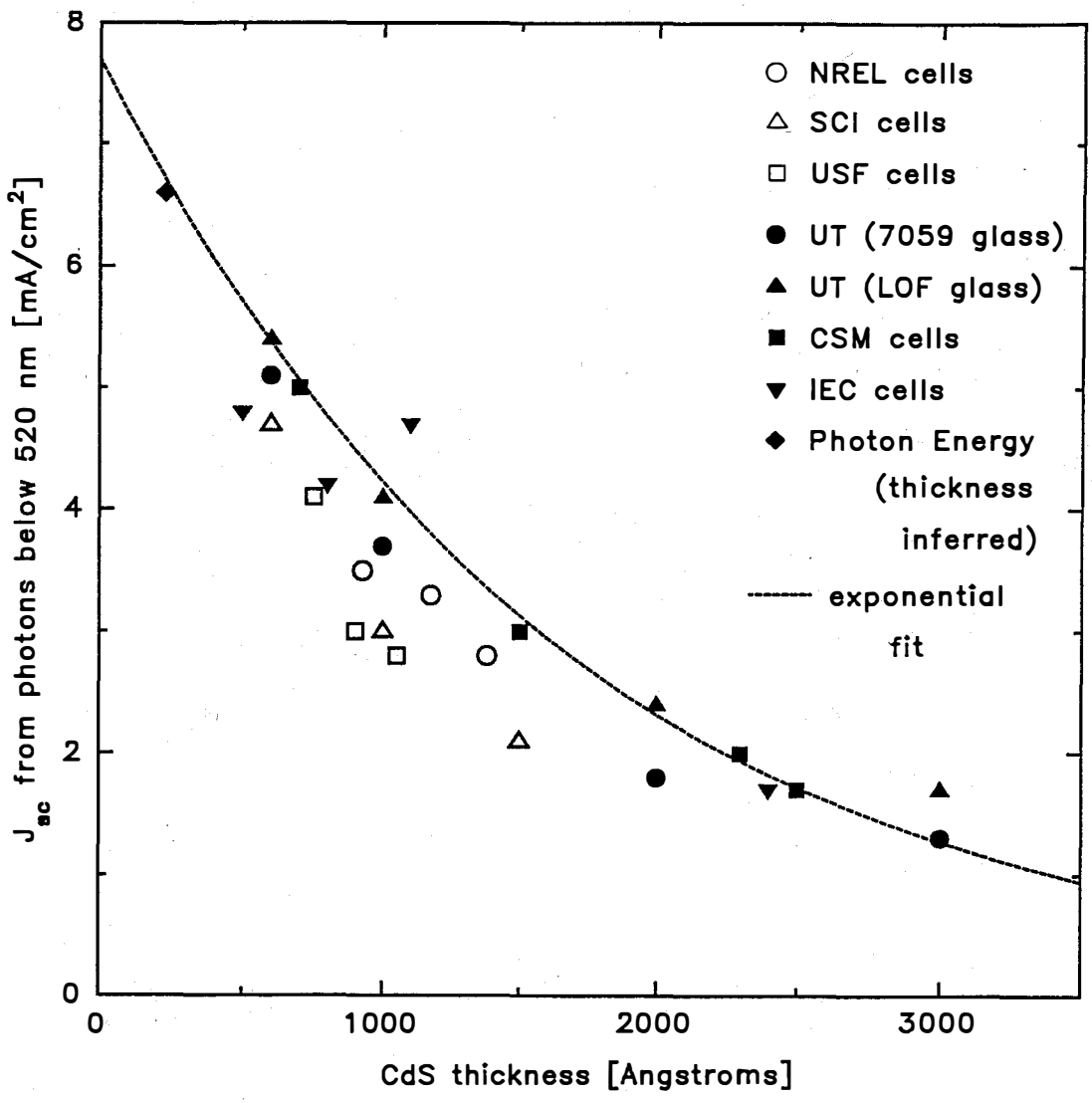

Figure 2. Variation with CdS thickness of photocurrent due to photons with energy exceeding CdS bandgap.

a CdTe cell to date. The CdS thickness in this case was not reported, but was described informally as very thin. Note in Fig. 2 that the practical range for short–wavelength collection, excluding the PE cell, covers about 4 mA/cm^2, from just over 1 to just over 5 mA/cm^2. This range might well

correspond to total photocurrents varying from 20 to 24 mA/cm, or efficiencies from 12.5 to 15%, assuming other parameters are unchanged.

For the cells in this study, other parameters were not always unchanged. In particular (see Fig. 3), below 1000 Å, V_{OC} decreased sharply in two cases, and fill factor in an additional two. The cells fabricated by NREL and USF did not show these decreases, but their thicknesses were all 800 Å and above. The earlier PE cell, however, with an inferred CdS thickness near 200 Å had V_{OC} = 790 mV and ff = 0.62, both values consistent with other PE cells made in that time frame. Thus, there is an existence proof that V_{OC} at least can be maintained when CdS is made quite thin.

Other parameters measured in the comparative study did not show systematic trends as CdS thickness was varied. The bandgap cutoff in the quantum efficiency was essentially the same for all CdTe cells studied. The capacitance showed variations in CdTe thickness between fabrication laboratories, but no discernable effect of CdS thickness. Series resistance and discernable shunting varied significantly from sample to sample, but these parameters also did not appear to be systematically affected by CdS thickness.

Band Offsets

There is growing experimental [2] and theoretical [3] evidence that there may be a significant conduction–band offset between $CuInSe_2$ and CdS. The impact on the performance of a CIS cell should be calculable, and several cases have been evaluated by Xiaoxiang Liu using the ADEPT software developed at Purdue University. In general (see Fig. 4), one finds a relatively broad range of band offsets that have only minor impact on current–voltage curves [4]. Room–temperature efficiency does fall rapidly for positive (Type I) offsets of 0.4 eV and above and somewhat more gradually for negative (Type II offsets) below –0.4 eV. These decreases are primarily due to distortions in the J–V curve, which correspond to significant decreases in fill factor. The range of band offset with minor practical impact is roughly proportional to absolute temperature. The current best guess of about 0.3 eV should have little effect at room temperature, but could become significant at reduced temperatures. Inclusion of a thin In–rich CIS surface layer has only a minor impact on these results.

Figure 4 makes the traditional assumption that most depletion, and hence band curvature, takes place in the CIS absorber as shown in Fig. 5. This assumption is valid as long as the CdS is relatively thin (0.1 μm) or more heavily doped than the CIS. There are situations, however, where those

assumptions cannot be made, either because there is a low carrier–density CdS layer of sufficient thickness or because a second offset between the transparent contact layer and CdS shifts additional

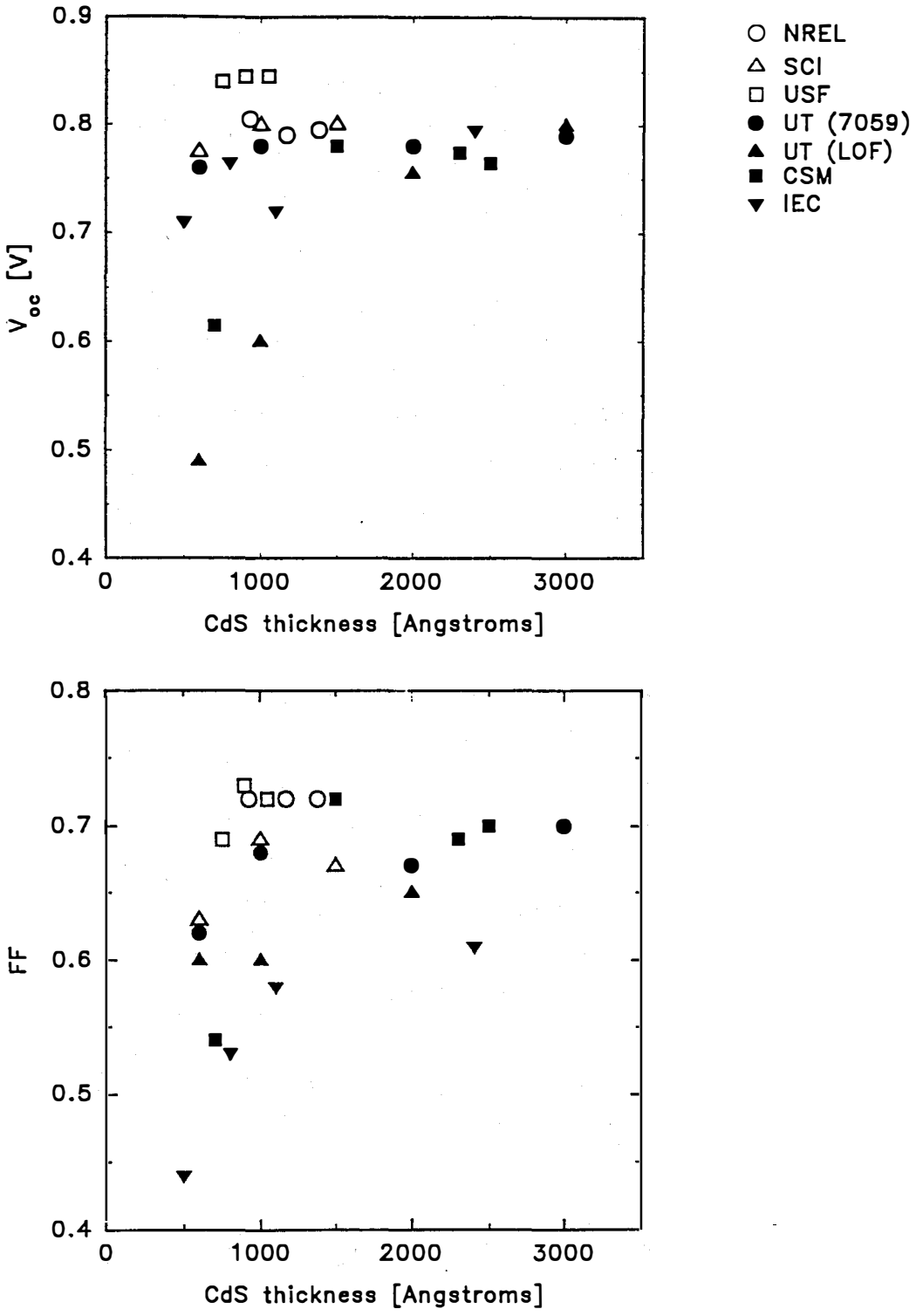

Figure 3. Values for V_{OC} and ff as a function of CdS thickness.

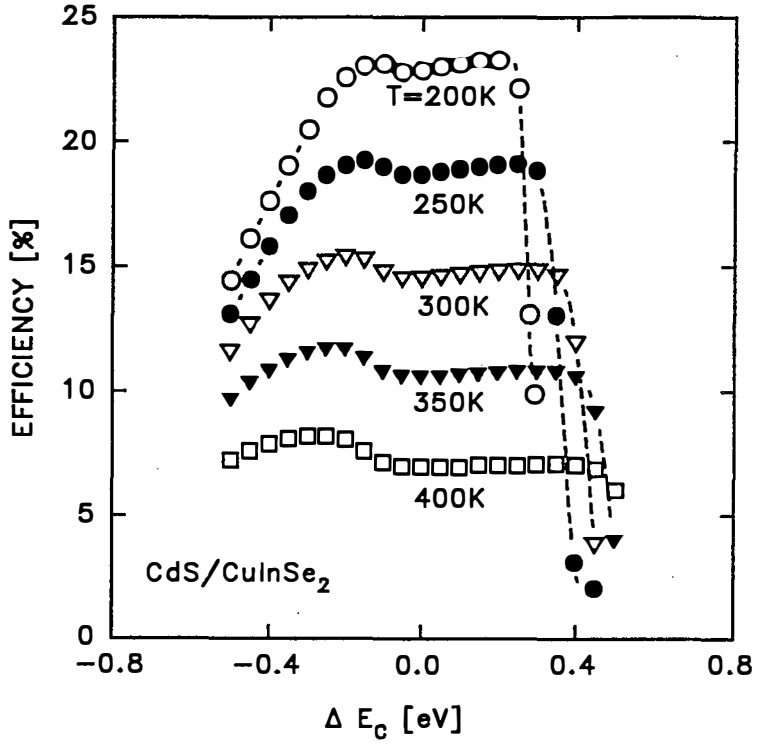

Figure 4. Calculated dependence of CIS efficiency on conduction–band offset. Parameters chosen are typical of high–quality cells. Positive offsets correspond to Type I.

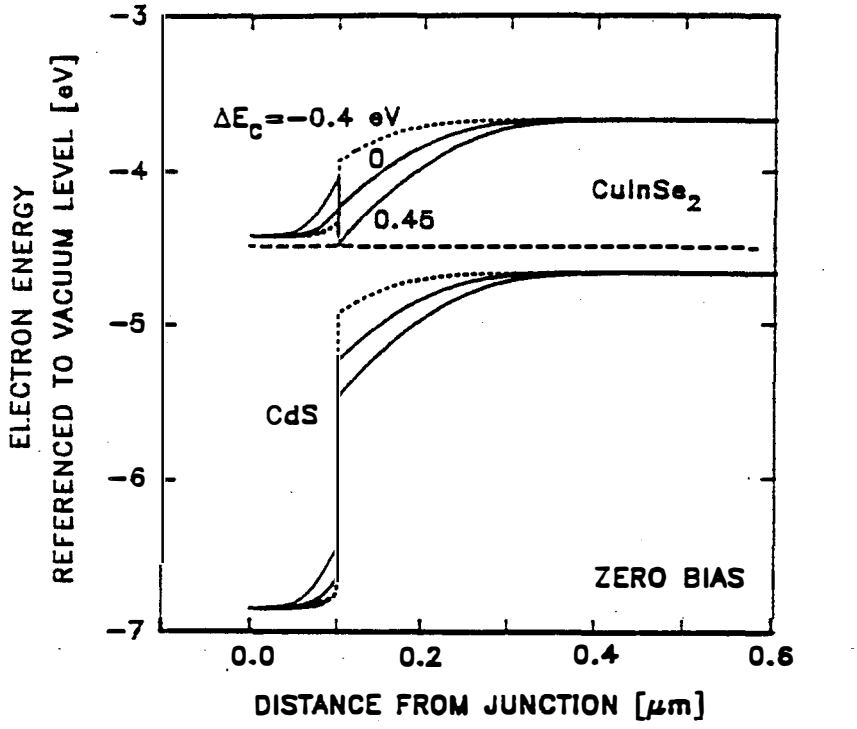

Figure 5. Calculated band–structure of CdS/CIS with some parameters used for Fig. 4.

depletion away from the absorber [5]. An example calculated by Ingrid Eisgruber is shown in Fig. 6. The curve marked n^-–CdS is a calculation based on low carrier–concentration material 0.1 μm thick, plus an assumed negative (Type II) conduction–band offset between the transparent ZnO contact and the CdS. In this case, the highest part of the conduction band, especially in forward bias, occurs in the CdS and there is effectively a second barrier to electron flow. With increased carrier–density CdS, labeled n, the extra structure has less impact on electron transport. Also shown in Fig. 6 is the nearly negligible effect of an indium–rich CIS surface layer.

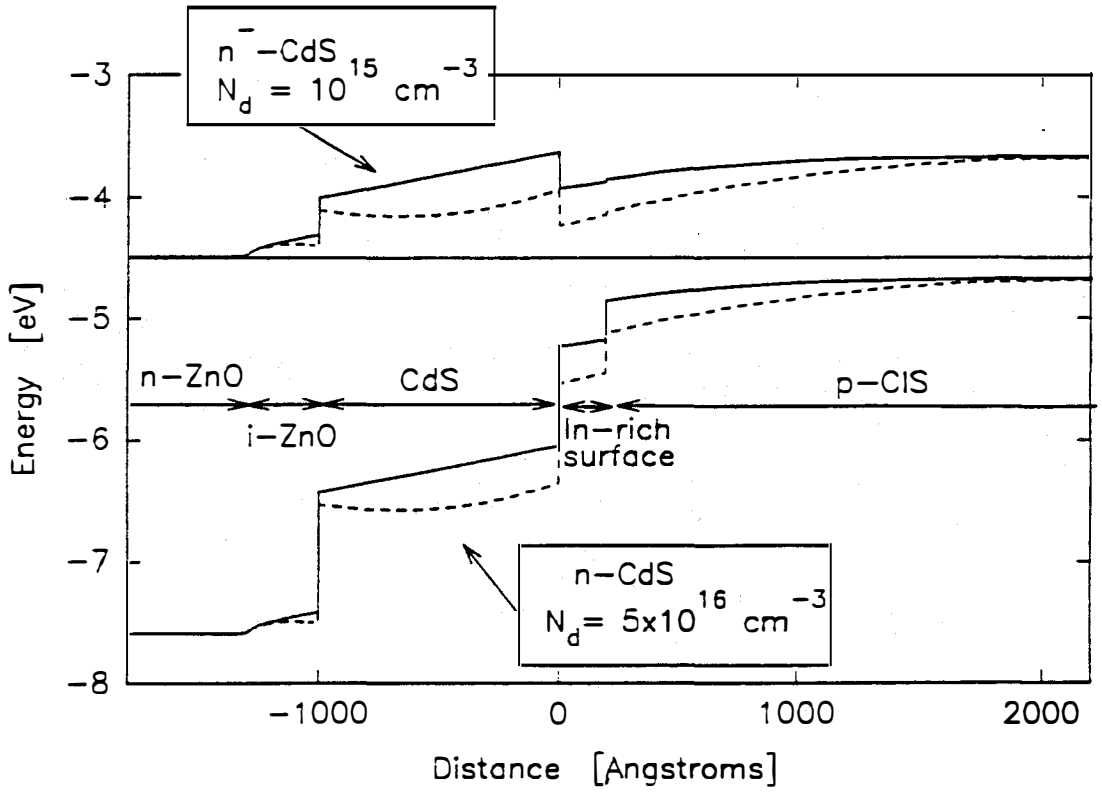

Figure 6. Calculated ZnO/CdS/CIS band structure contrasting n and n^- CdS.

The light and dark J–curves resulting from the two types of CdS used for the Fig. 6 band diagrams are shown in Fig. 7. Note the major distortion of the light n^-–curve, which has the appearance of a light and a dark diode of the same polarity in series. The secondary diode would increase the turn–on voltage in the dark, but not significantly affect V_{OC} in the light. Such curves are not uncommon experimentally. In fact, some cells show a transition from the n^-–curves to the n–curves when exposed to light containing blue photons, and subsequent relaxation over several hours when the blue photons are removed [5]. Other cells retain the distortion, though the blue light may lessen

it somewhat. There is probably some selectivity in reporting, so that the distorted curves may be more prevalent than generally realized.

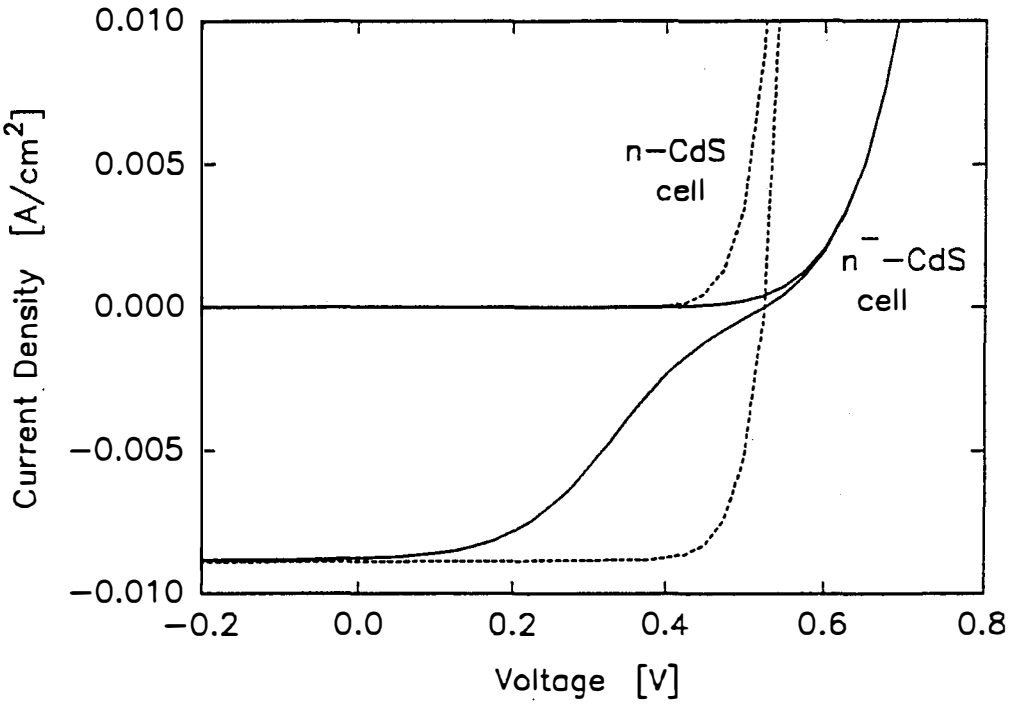

Figure 7. Calculated light and dark J–V curves for the n and n^- CdS shown in Fig. 6.

The proposed explanation for an n– to n^-– transition, shown in Fig. 8, is a modification in the occupation of deep CdS states. Figure 8a shows n–CdS without deep levels, where the n–type behavior is due to ionization of shallow donor states. The n^-–CdS case is attributed to a density of acceptor–like deep states comparable to the donor density. These deep acceptor states trap most of the free electrons contributed by the donors. The resulting low free electron concentration is shown in Fig. 8b. The effect on the J–V curves will be greatest when the n^-–CdS (plus any low–carrier density ZnO) is relatively thick. When incident photons are absorbed in the CdS (i.e., blue photons), the concentrations of both free electrons and free holes increase greatly, and many of the deep levels are now occupied by light–generated holes, as shown in Fig. 8c. If these deep levels are long–lived, the CdS will remain in the configuration for an extended time, and one will have effectively photoinduced a transition from n^-–CdS (few free electrons) to n–CdS (many free electrons). The long relaxation times observed after the illumination is removed can be attributed to the slow discharging of the deep traps. Furthermore, the necessity to have photons with energy greater than the CdS bandgap is clearly verified by the separate experiments shown in Fig. 9 where monochromatic light of varying wavelength was employed.

If standard light conditions remove the extraneous "n^-" features shown in Fig. 7, one might argue that cell performance is not degraded. However, such cells would be located in parameter space close to major performance problems, and it would probably be wise to use information such as Fig. 7 as a indicator of potential trouble if there is some variation in processing.

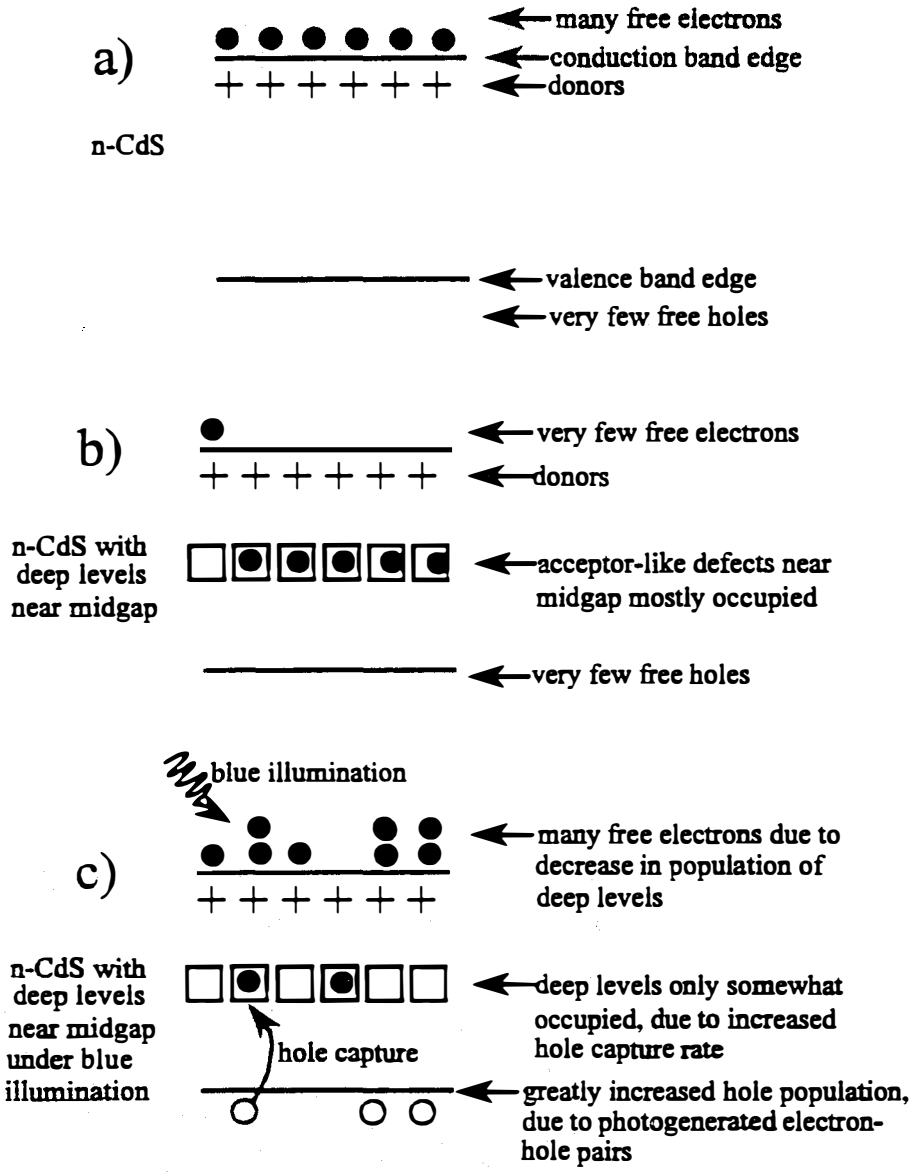

Figure 8. Carrier populations in (a) n–type CdS, (b) n–CdS with deep levels, and (c) no CdS with deep levels under deep illumination.

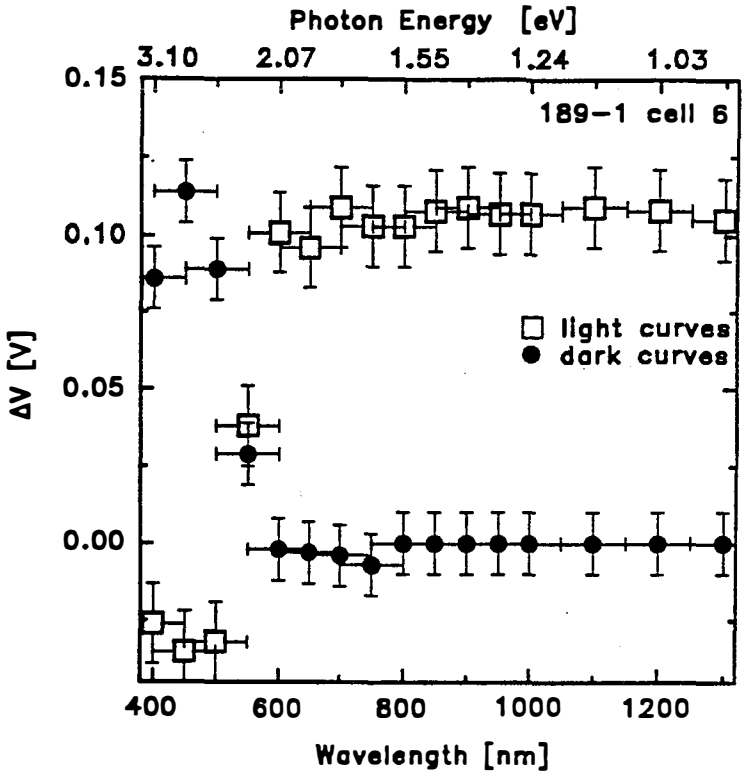

Figure 9. Voltage shift in dark J–V curve before and after monochromatic illumination, and in monochromatic J–V curves before and after white–light illumination.

Specific Projects

In addition to the cell–level results described above, we worked closely with three industrial groups on investigations specific to their issues. A listing of individual reports prepared is given in the Communications section.

CdTe. An obvious optical investigation for CdTe cells is to compare the optical losses for different glass/TCO combinations. John Sharp measured absorption, reflection, and thicknesses from a number of superstrate combinations supplied by Solar Cells, Inc. This data was then used to calculate the photocurrent losses to be expected, and hence give a quantitative basis for evaluating different CdTe superstrates.

CIS/CIGS. Incorporation of gallium in selenized CIS layers has been a challenge, but during 1995, ISET was relatively successful in making expanded bandgap CIGS cells. Jon Sharp assisted with characterization of cell losses, establishing the doping profile, and a comparison of bandgaps determined by quantum efficiency and V_{OC} vs. T. This work has been submitted for publication

with joint ISET, CSU, and NREL authorship [6]. In another joint project, Jennifer Granata investigated a number of CIS cells in the 11–14% efficiency range fabricated by Siemens Solar Industries. Here also careful measurements were used to deduce and compare the individual cell parameters. Finally I worked with the NREL CIS group to explore the resulting cell structure when CIS was deposited on CGS of varying thickness [7].

References

[1] R. A. Sasala, X. X. Liu, and J. R. Sites, "Comparative Analysis of Recent High–Efficiency CdTe Solar Cells," Int. J. Solar Energy **12**, 17 (1992).

[2] D. Schmid, M. Ruckh, and H. W. Schock, "A Comprehensive Characterization of the Interfaces in Mo/CIS/CdS/ZnO Solar Cell Structures," Proc. WCPEC **1**, 198 (1994).

[3] S. H. Wei and A. Zunger, "Band Offsets at the CdS/$CuInSe_2$ Heterojunction," Appl. Phys. Lett. **63**, 2549 (1993).

[4] X. X. Liu and J. R. Sites, "Calculated Effect of Conduction–Band Offset on $CuInSe_2$ Solar–Cell Performance," AIP Conf. Proc. **353**, 444 (1995)

[5] I. L. Eisgruber, J. E. Granata, J. R. Sites, J. Hou, and J. Kessler, "Blue–Photon Modification of Nonstandard Diode Barrier in $CuInSe_2$ Solar Cells," submitted to J. Appl. Phys.

[6] B. M. Basol et al., "Cu(In,Ga)Se_2 Thin Films and Solar Cells Prepared by Selenization of Metallic Precursors," Solar Energy Materials and Solar Cells, in press.

[7] B. M. Keyes et al., "The Influence of Ga on the Properties of CuIn(Ga)Se_2–Based Thin Films and Devices," Proc. 11th ICTMC Conf., Stuttgart (1995).

MODULE ANALYSIS

Cell Geometry

Individual cells in a monolithic thin film module typically have a width of 0.5 to 1.0 cm and no grid fingers. Hence, the effective series resistance, with typical transparent oxide front contacts, is 2–5 Ω–cm^2, which leads to a 10–20% reduction in fill factor efficiency at 100 mW/cm^2. Actual loss in the field is perhaps only half this amount, since average solar illumination is likely to be closer to 50 mW/cm^2 [8].

Of additional concern for analysis purposes is failure of the single–parameter series–resistance model due to a significant voltage drop across the top contact of each cell [9]. Figure 10 contrasts J–V curves light and dark J–V curves calculated with a large single–parameter series resistance with that

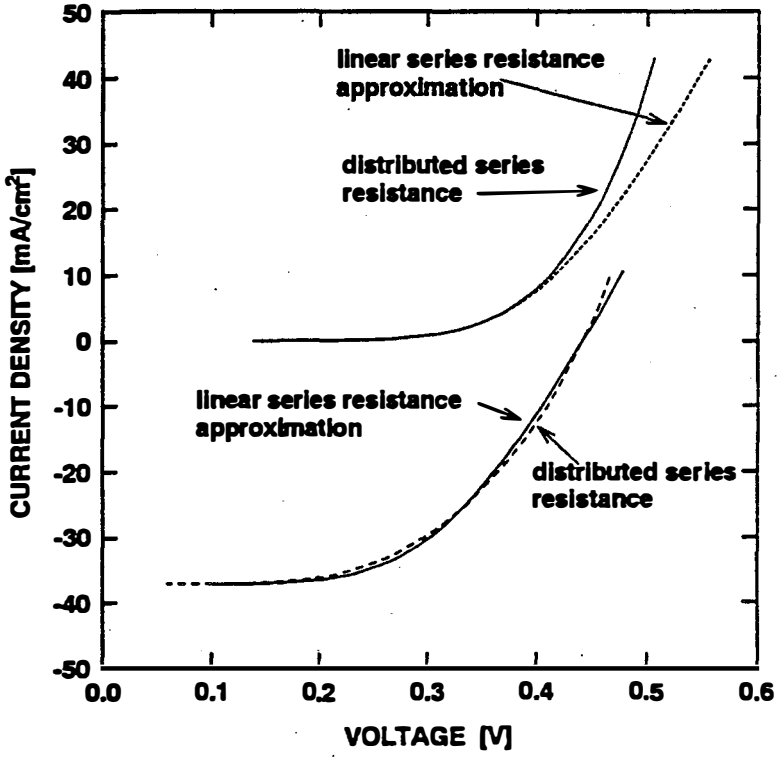

Figure 10. Calculated curves for a CIS cell assuming a 1–cm width and a sheet resistance of 7.6 ohms per square.

done more carefully with the proper voltage distribution across the cell. The maximum power point is not much affected, but the diode quality factor is significantly overestimated in the single series–resistance approximation. Subsequent reduction in sheet resistance can therefore be misidentified as an improvement in diode quality factor. Furthermore, the single series–resistance approximation will exaggerate light/dark differences in quality factor and series resistance.

Encapsulated Modules

Laser–scanning, or OBIC, measurements can be very valuable in identifying defects in both individual cells and modules. There is a difficulty, however, with analyzing encapsulated modules where the cells cannot easily be contacted individually. At dc or low frequency, the OBIC signal is proportional to the photocurrent/shunt–resistance product. At high frequency, however, the photocurrent is scaled by inverse capacitance, which is generally more uniform than shunt resistance. Ingrid Eisgruber has developed a technique to separate photocurrent and shunt resistances with measurements at two frequencies, even when the higher one is well below the high frequency limit [10]. Figure 11 shows the measured signal from a 14–cell module at three different frequencies, plus the fit based on the deduced shunt resistance for each cell.

The photocurrent/shunt–resistance separation technique has been applied to CIGS, CdTe, and a–Si modules. In Figs. 12–14, an example of the results from each is shown. In these cases, the OBIC signal has been converted to quantum efficiency for each cell at the 633 nm wavelength of the laser used. For the CIGS and CdTe modules, there is very good agreement between the shunt resistance and quantum efficiencies deduced from the laser scan and those measured directly from the individual cells. For these modules, the spread in shunt resistance is a factor of two or less. The a–Si module, however, had a cell–to–cell variation in shunt resistance of two orders of magnitude. The agreement of the values deduced from the laser scan with those measured directly was not as good, but still quite respectable given the huge variation in shunting.

Forward Bias

Additional information from laser scanning can be acquired when cells are placed in forward bias. Figure 15 illustrates that variations in series resistance are not observed at zero bias, but are if a cell is forward biased. The apparent quantum efficiency (AQE) is reduced from the zero–bias value by the ratio of the two solid arrows in Fig. 15 and can thus be calculated from the light and dark J–V curves.

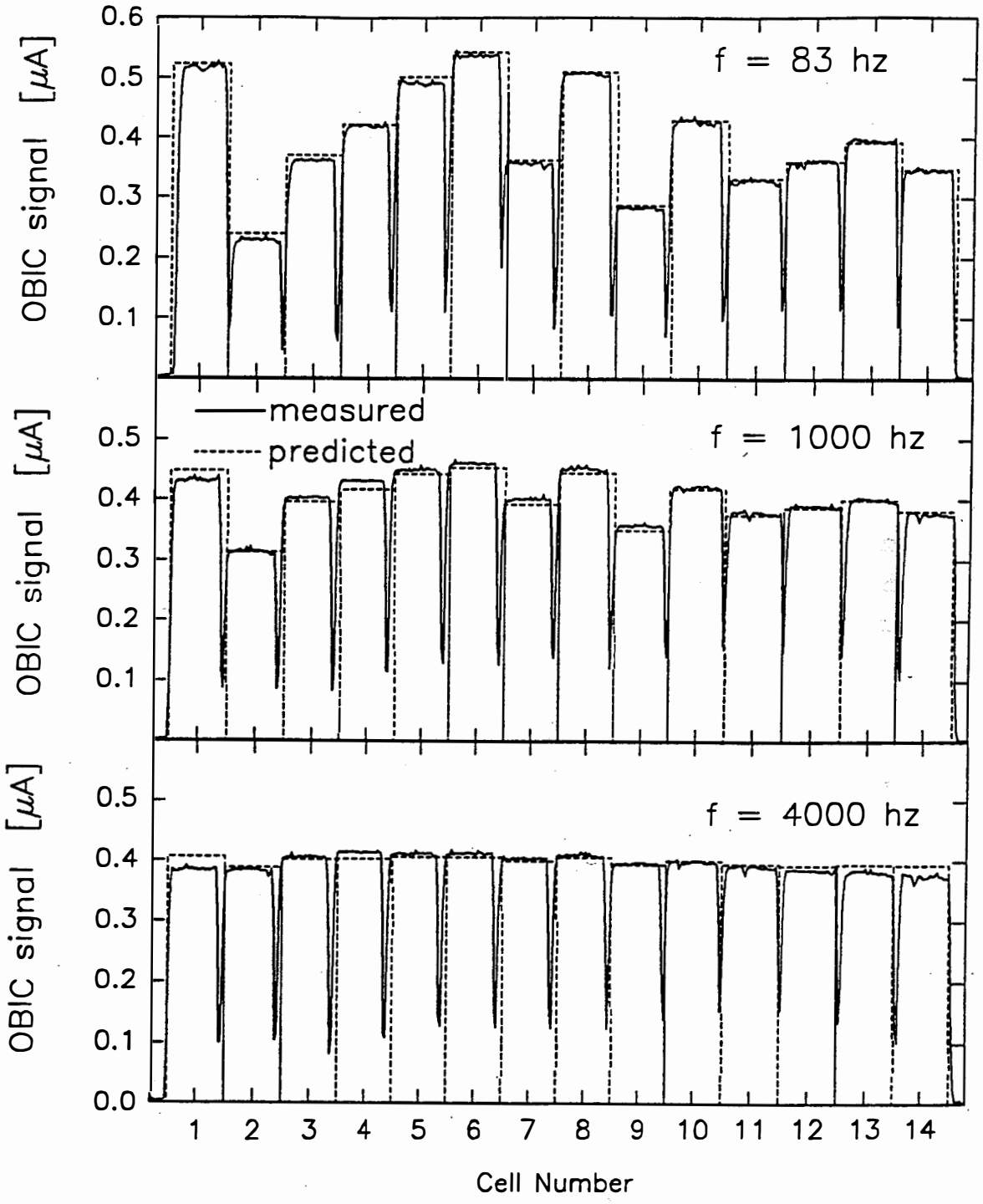

Figure 11. Measured and calculated line scans at different frequencies for a small CIGS module.

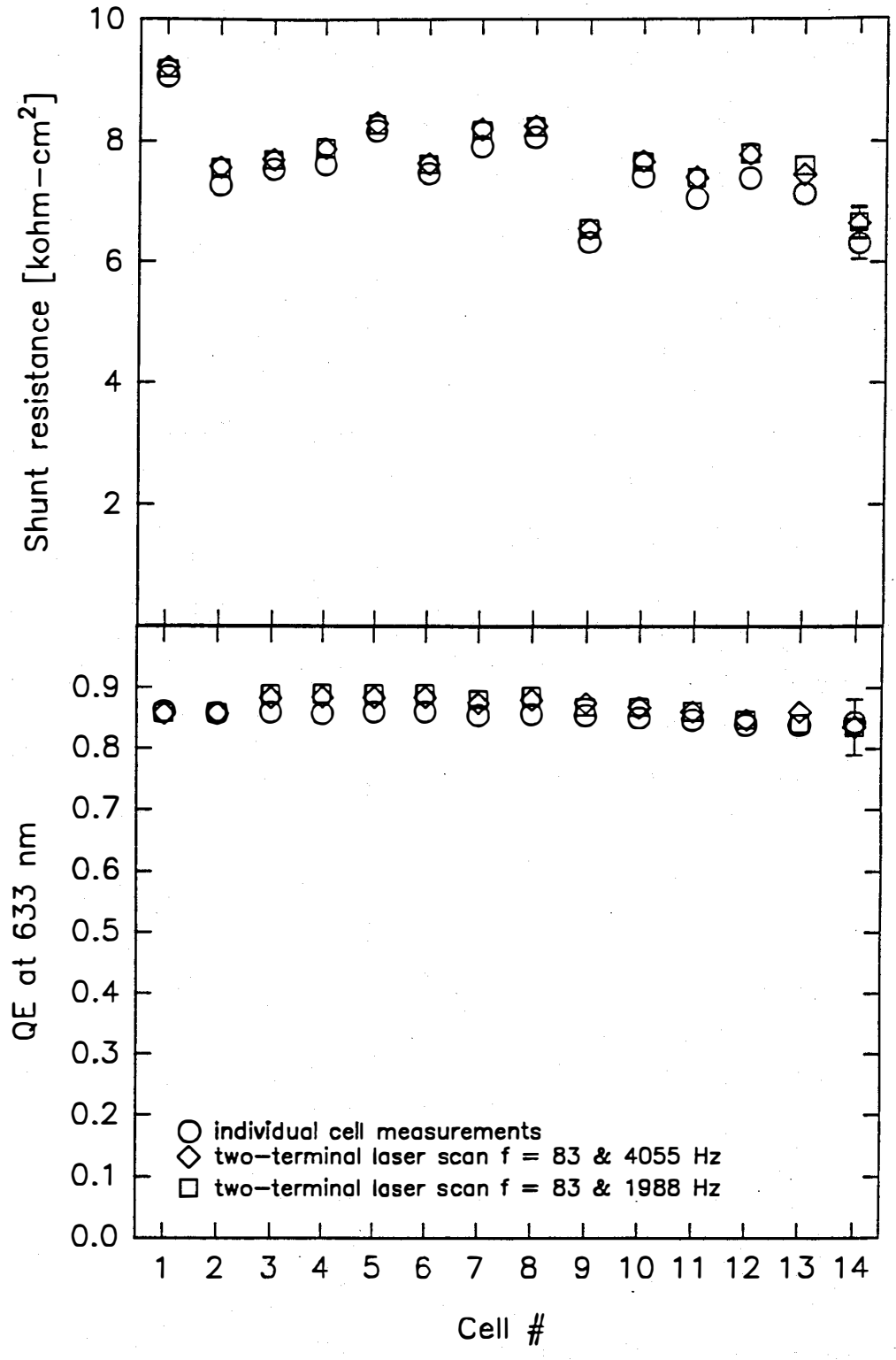

Figure 12. Comparison of CIGS mini–module shunt resistance and quantum efficiency deduced from two–terminal line scans with that measured directly.

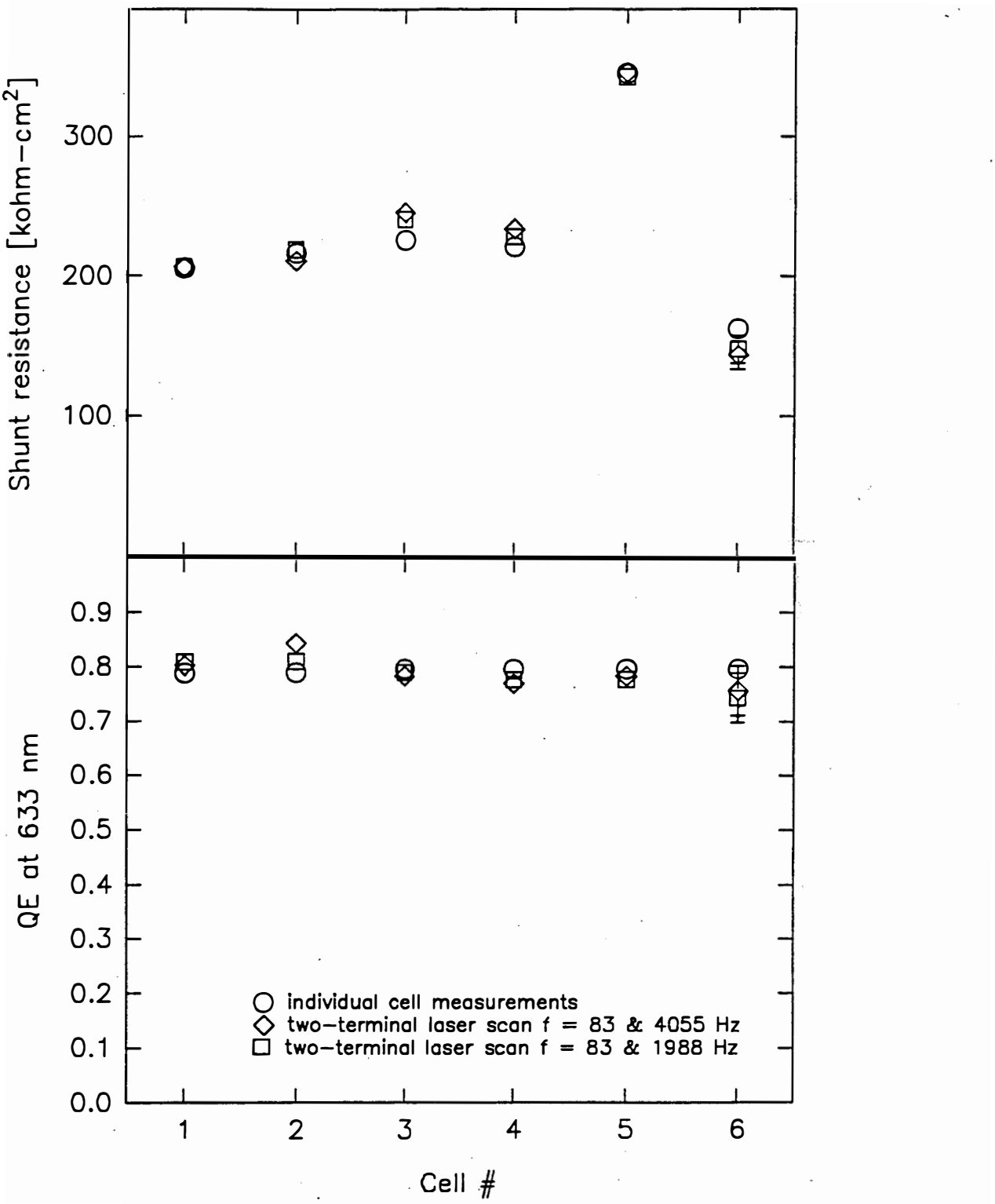

Figure 13. Comparison of CdTe mini–module shunt resistance and quantum efficiency from two–terminal line scans with that measured directly.

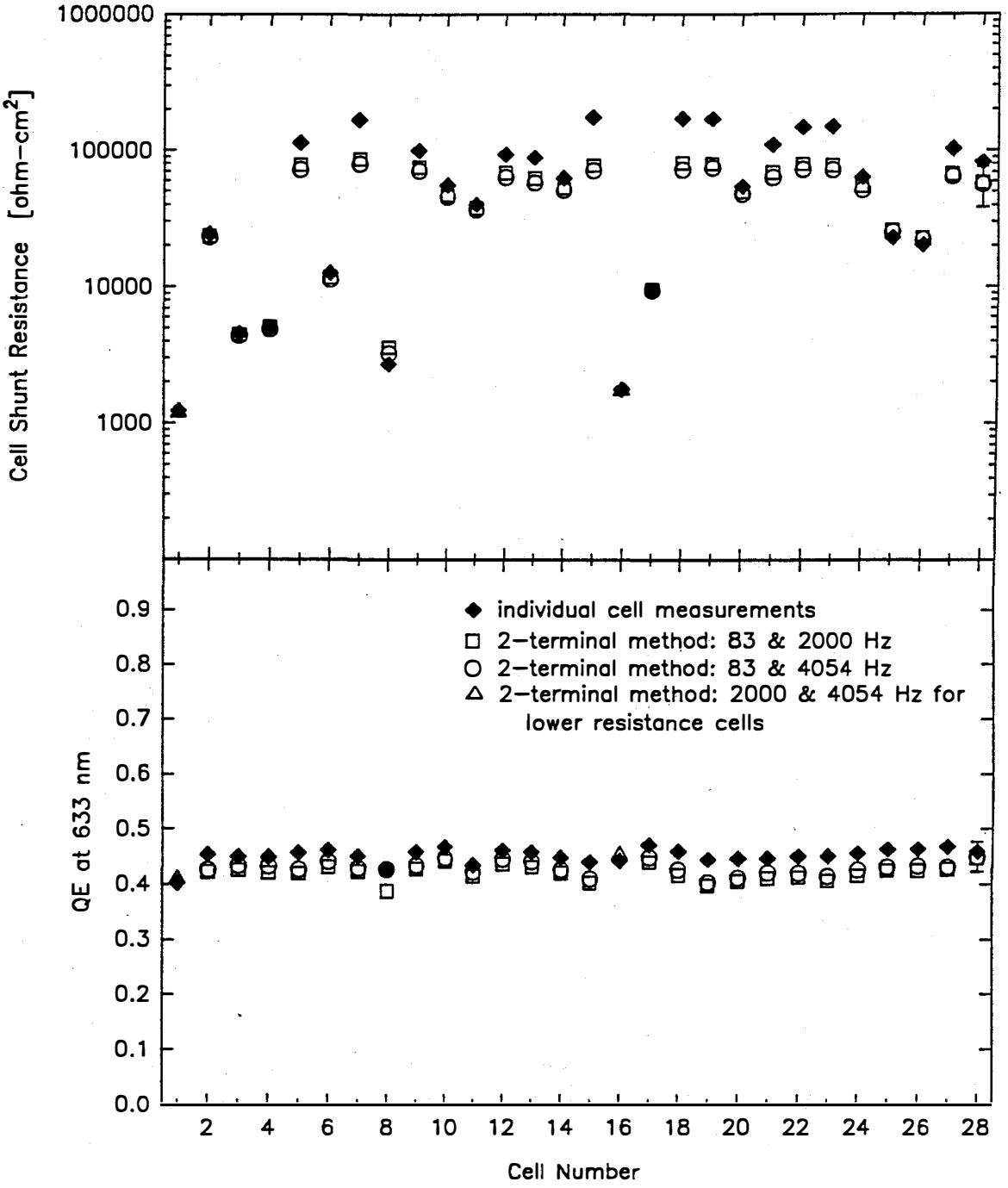

Figure 14. Comparison of α–Si module shunt resistance and quantum efficiency deduced from two–terminal line scans with that measured directly.

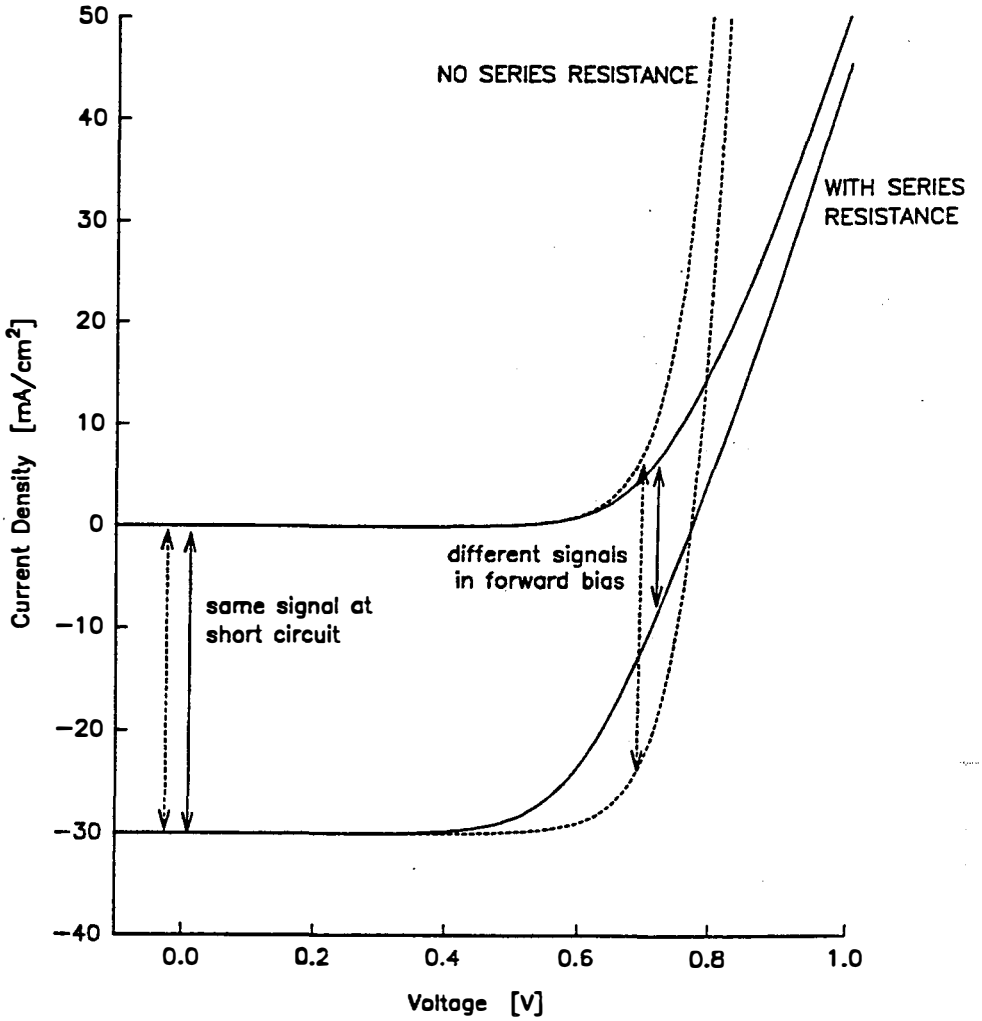

Figure 15. Contrast of short–circuit and forward–bias laser scans for cells with and without series resistance.

Figure 16 shows how AQE varies with series resistance and light intensity for a forward bias between V_{MP} and V_{OC}. If other cell parameters are assumed to be fixed, variations in one parameter across the cell can be deduced. Forward–bias scans can therefore be used to identify regions of varying resistivity in $CuInSe_2$ and CdTe cells as shown in Fig. 17. It is necessary to select voltage bias and scan intensity so that the plot shown in Fig. 16 is relatively sensitive to series resistance. The top scan of Fig. 17 was done at zero bias and a laser intensity comparable to two suns, conditions where AQE is insensitive to series resistance. As expected, it is quite uniform. At forward bias, however, the signal drops by varying amounts depending on the local resistivity. The drop is greater when the forward current is greater (lowest trace), and it is also present at higher laser intensities, which drive the diode locally into forward bias (9500 mA/cm^2 trace).

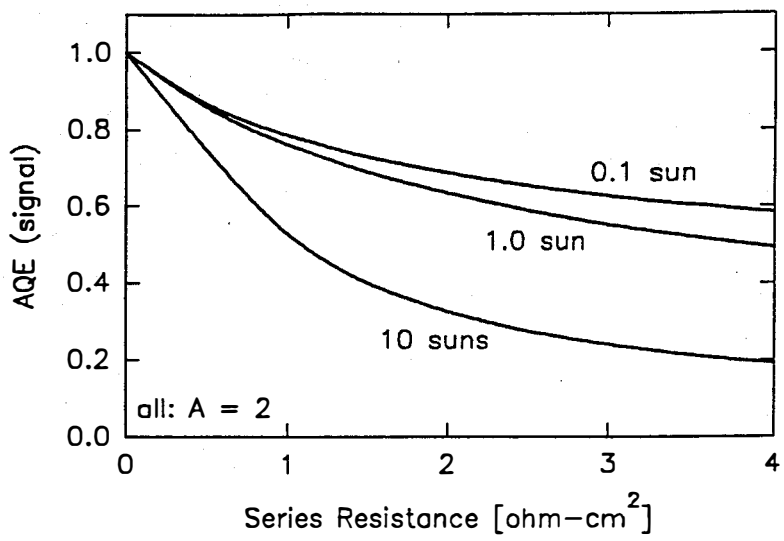

Figure 16. Laser–scan signal vs. series resistance for a typical CdTe cell at 0.74 V forward bias.

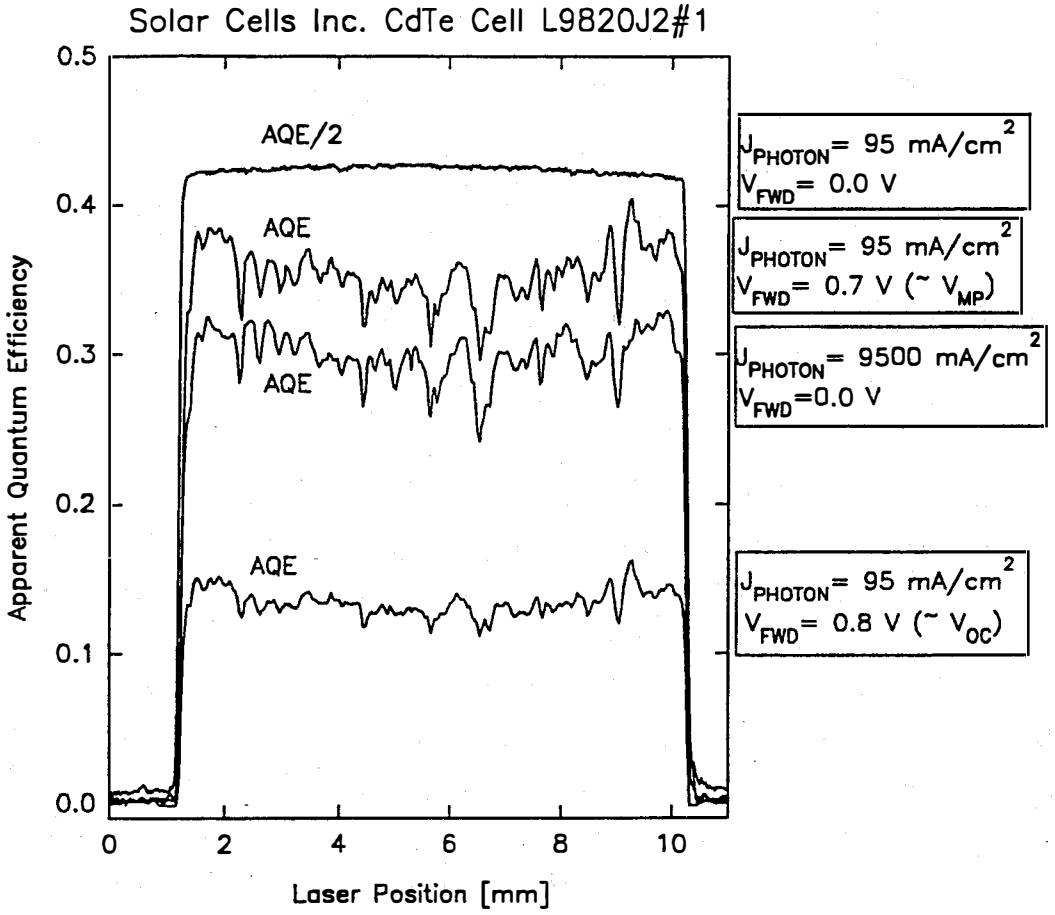

Figure 17. Line scans of a CdTe module cell at different voltages and intensities.

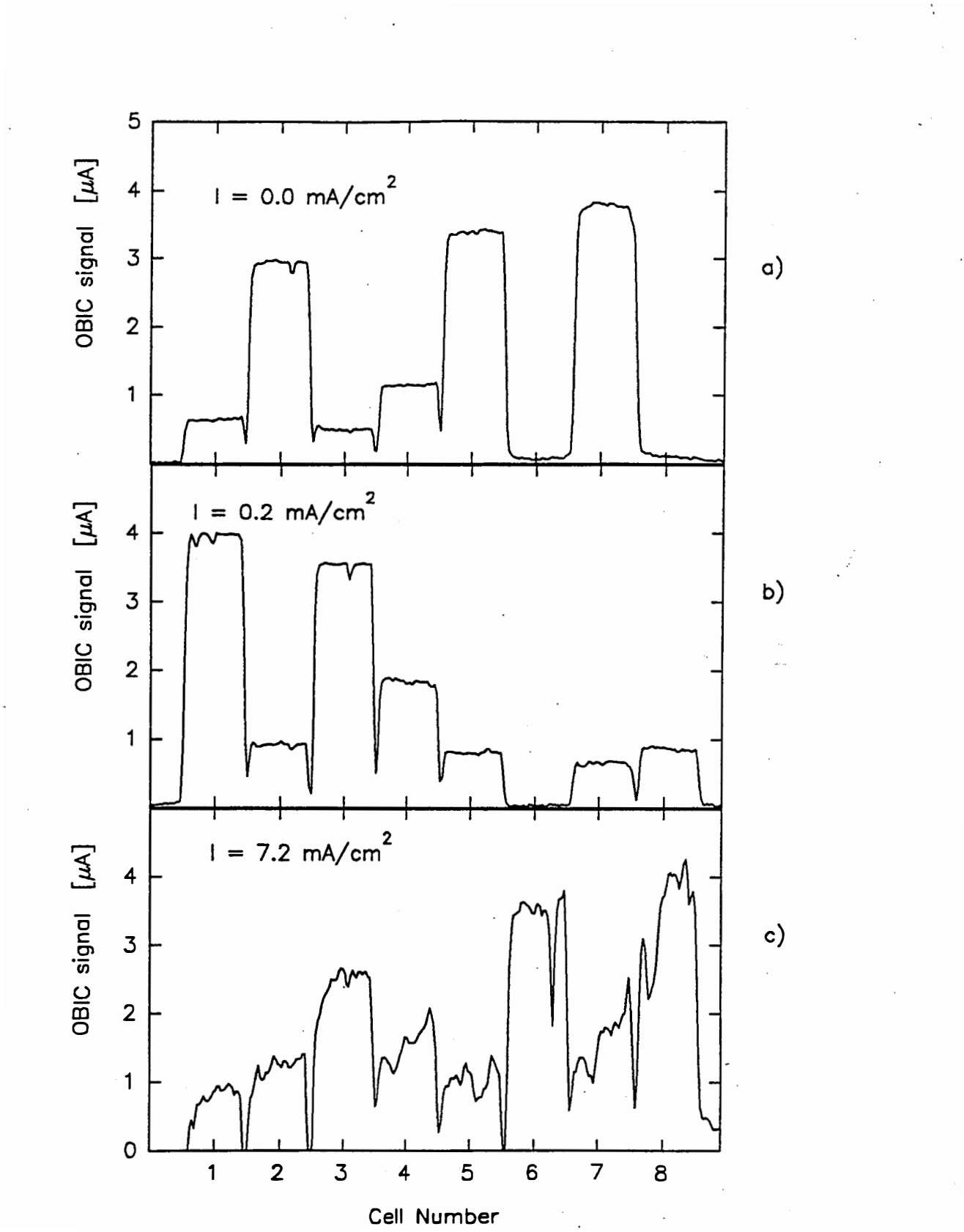

Figure 18. Line scans from a CdTe mini-module at (a) zero bias, (b) modest forward bias, and (c) somewhat larger forward bias.

Forward bias is also useful for a rough estimate of the leakage in severely shunted cells, where the zero–bias OBIC signal is essentially zero for all accessible frequencies. If bias is increased, however, the leaky cells eventually acquire a signal comparable to the other cells. In Fig. 18a, cells 6 and 8 clearly have a low shunt resistance compared to the other cells. With forward bias sufficient for a small forward current (Fig. 18b), the cell–8 signal becomes comparable to the others, and at a significantly higher forward current (Fig. 18c), cell 6 does the same. Calculation shows cell 8 has a shunt resistance of about 400 Ω–cm^2 and cell 6, about 10 Ω–cm^2. All the other cells have shunt resistances over 3000 Ω–cm^2. Note that local series resistance features similar to those seen in Fig. 17 are present in the 18b and 18c forward–bias scans.

Non–Uniformities/Bias Light

Illumination variations over a module lead to current generation, limited by the least illuminated cell, and temperature variations along a cell lead to a voltage limited by the highest temperature, or lowest voltage, region. Illumination variations, however, will additionally seriously distort a laser scan across a module if one attempts bias–light measurements. This point is illustrated in Fig. 19. The top scan, done without bias, light shows the variations with shunt resistance discussed earlier. In the presence of uniform light bias, this pattern should not change. If, however (Fig. 19b), even relatively weak white–light bias with a modest spatial variation is applied, the pattern changes dramatically. Hence, bias light is not recommended for module laser scans.

EVA Browning

A small laser–scanning project involving crystalline–silicon module was also undertaken by Ingrid Eisgruber. Browning of the ethyl vinal acetate (EVA) encapsulant commonly used for silicon modules has been observed for sometime. Laser scanning, however, shows quite clearly that the field browning is a single transition, i.e., individual regions of the module are either browned or not–browned. The red (633 nm) quantum efficiency drops a small amount from 81 to 77% and the blue (488 nm) considerably more from 57 to 37% in qualitative agreement with the results reported by Pern [11]. The browning appears to usually begin at a major bus–bar, then propagate outwards with an interface that is abrupt on a scale much less than a millimeter.

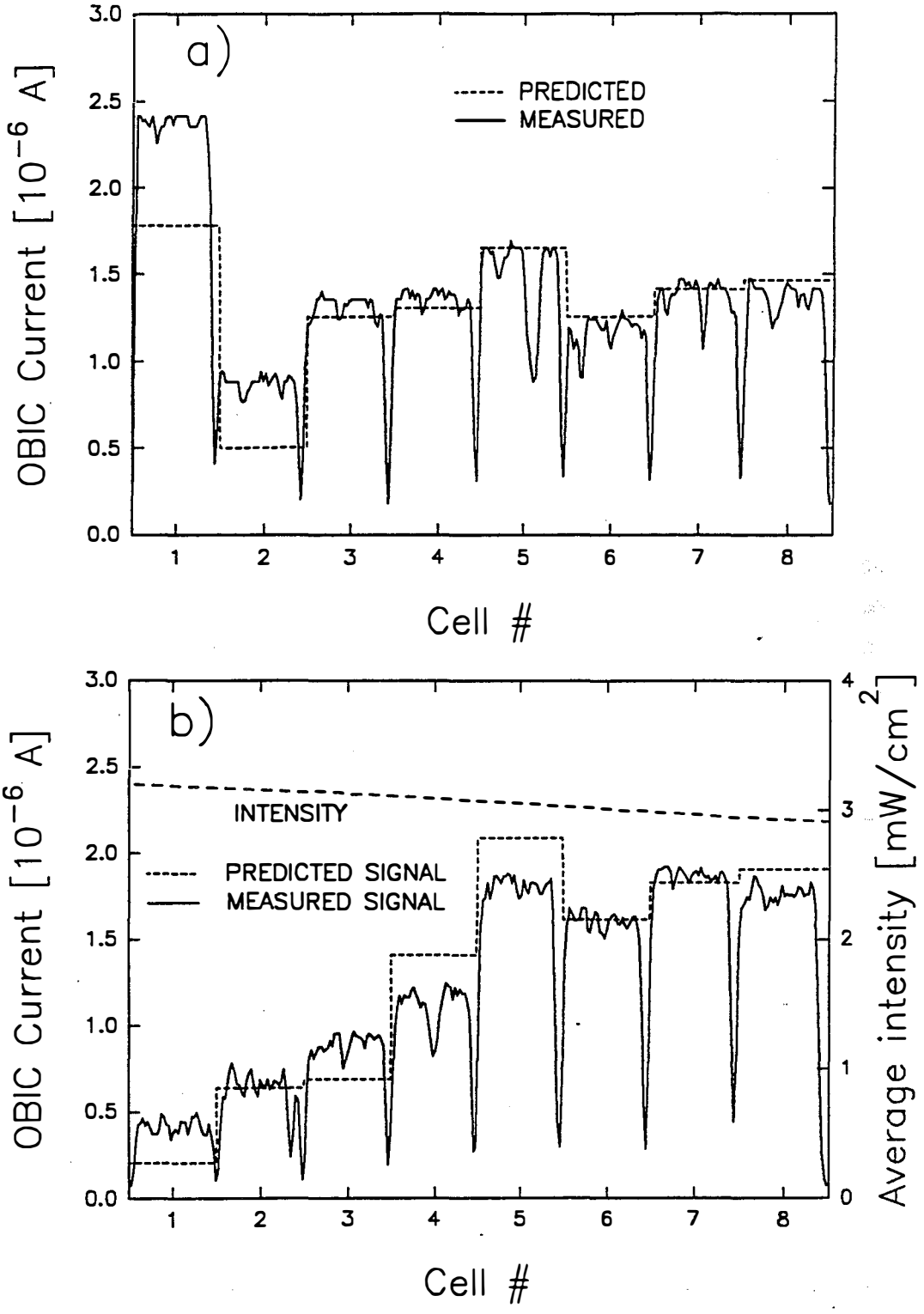

Figure 19. Short–circuit line scans from a CdTe mini–module without light bias (a) and with modest white light bias (b).

References

[8] A. Delahoy, "Energy Delivery for Various PV Technologies Based on Realistic Irradiance and Temperature Distributions: Implications for Module and System Design," Proc. EPSECE **13**, 1474 (1995).

[9] I. L. Eisgruber and J. R. Sites, "Effect on Thin–Film Module Geometry on Solar–Cell Current–Voltage Analysis," Proc. WCPEC **1**, 271 (1994).

[10] I. L. Eisgruber and J. R. Sites. "Extraction of Individual–Cell Photocurrents and Shunt Resistances in Encapsulated Modules Using Large–Scale Laser Scanning," **4**, 63 (1996).

[11] J. F. Pern, "Factors that Affect the EVA Encapsulant Discoloration Rate Upon Accelerated Exposure," Proc. WCPEC **1**, 897 (1994).

TEAM ACTIVITIES

The Colorado State program has been quite active in both the CdTe and CIS teams organized as part of the NREL Industrial Partners initiative. I have participated in all the team meetings to date, and have brought in the research students when appropriate.

CdTe

Jennifer Granata and I have been active participants on the CdTe Device Team. Our primary project was described earlier in the section on CdS thickness, where we did optical and device measurements on CdTe cells prepared by six laboratories. We gave one major report at the team meeting in May 1995, and we are preparing a second for the team meeting in January 1996.

CIS

I have been serving as team leader for the CIS Junction Team and have been working with NREL staff on meeting logistics. Specific junction–team activities have been the initiation of electronic communications, careful characterization of CIS or CIGS from several laboratories, exploration of different absorber surface treatments during the formation of the window layer, and consideration of junction analysis techniques that might be amenable to in situ diagnostic information. Perhaps the biggest accomplishment of the CIS team as a whole, however, has been the bringing together of all the major U.S. players to discuss their common issues.

RECOMMENDATIONS

The first recommendation is for the community to become more proactive in bridging the gap between research–level cells and large modules. This is probably best done with what has come to be called the mini–module: 6–8 cells connected in series by module–scribing techniques with total size of 10 cm × 10 cm, or somewhat less. Such structures should contain the same information as large modules, but are much more compatible with most characterization apparatus. Furthermore, it is generally practical to form individual test cells with near–identical processing to that used for the mini–modules.

A related recommendation is to more routinely save test structures after the completion of each layer of cell fabrication. Such structures have proven invaluable in separating the CdTe photon losses and nearly as useful in studying the electronics and morphology of CIS cells.

The final, and probably most important, recommendation is to actively support and nurture the teaming process. There may be setbacks, and the successes may come by roundabout paths, but the potential synergy is quite high, and the incremental cost is quite modest. Specifically, the team process is well matched to interlaboratory comparisons, systematic variations in device features, and exchange of minimally–filtered data within the community.

COMMUNICATIONS

Publications

1. J. R. Sites and X. X. Liu, "Performance Comparison Between Polycrystalline Thin–Film and Single–Crystal Solar Cells," Prog. in Photovoltaics **3**, 307 (1995).

2. J. R. Sites and X. X. Liu, "Recent Efficiency Gains for CdTe and $CuIn_{1-x}Ga_xSe_2$ Solar Cells: What Has Changed?" Solar Energy Materials and Solar Cells, in press.

3. X. X. Liu and J. R. Sites, "Calculated Effect of Conduction–Band Offset on $CuInSe_2$ Solar–Cell Performance," AIP Conf. Proc. **353**, 444 (1995).

4. I. L. Eisgruber and J. R. Sites, "Extraction of Individual–Cell Photocurrents and Shunt Resistances in Encapsulated Modules Using Large–Scale Laser Scanning," Prog. Photovoltaics **4**, 63 (1996).

5. B. M. Keyes, J. Tuttle, J. Sites, A. Tennant, S. Asher, M. Conteras, K. Ramanathan, A. Gabor, J. Webb, R. Ahrenkiel, and R. Noufi, Proc. 11th Int. Conf. on Ternary and Multinary Materials, 1995, xxx.

6. G. Stollwerck and J. R. Sites, "Analysis of CdTe Back–Contact Barriers," Proc. 13th European PV Solar Energy Conf., 1995, p. 2020.

7. B. M. Basol, V. K. Kapur, A. Halani, C. R. Leidholm, J. Sharp, J. R. Sites, A. Swartzlander, R. Matsen, and H. Ullal, "$Cu(In,Ga)Se_2$ Thin Films and Solar Cells Prepared by Selenization of Metallic Precursors,"J. Vac. Sci. Technol., Aug. 1996.

8. I. L. Eisgruber, J. E. Granata, J. R. Sites, J. Hou, and J. Kessler, "Blue–Photon Modification of Nonstandard Diode Barrier in $CuInSe_2$ Solar Cells," submitted to J. Appl. Phys.

Presentations

1.	PVAR8D	Denver	Liu	May 1996
2.	CdTe Team	Golden	Granata	May 1996
3.	NREL	Golden	Eisgruber	August 1996
4.	Performance/Reliability Workshop	Denver	Sites	September 1996

5. European Conference	Nice	Stollwerck	October 1996
6. Colorado State University	Fort Collins	Sites	Novermber 1996

Graduate Degrees

1. Gunther Stollwerck (May 1995), M.S. Thesis: "Quantitative Separation of Photon and Back–Contact Losses in CdTe Solar Cells."
2. Jon Sharp (May 1995), M.S. Coursework/Project Degree.

Specific Cell/Module Reports

Date	To	Done By	Topic
12/94	Solarex	Eisgruber	OBIC Primmer
1/03/95	Solarex/Kessler	Eisgruber	CIS Laser Scans
1/03/95	Siemens/Tarrant	Granata/Sites	CIS Measurements
1/10/95	SCI/Sasala	Eisgruber	Water White Glass
2/14/95	SCI/Sasala	Granata/Sharp	CdS Optics
2/22/95	Solarex/Kessler	Eisgruber	CIS Measurements
2/24/95	SCI/Sasala	Sharp	Rolled Glass Optics
2/27/95	Siemens/Tarrant	Granata/Sites	CIS Measurements
3/20/95	SCI/Sasala	Granata	CdS Optics
5/03/95	SCI/Sasala	Eisgruber	CdTe Module Scan
5/10/95	ISET/Basol	Sharp	Selenized CIGS
5/24/95	ISET/Basol	Sharp	Selenized CIGS
5/26/95	Siemens/Tarrant	Granata	CIS Measurements
6/08/95	SCI/Sasala	Eisgruber	CdTe Module Scan
6/09/95	ISET/Basol	Sharp	Selenized CIGS
6/30/95	SCI/Sasala	Murphy	Glass/TCO Optics
7/07/95	ISET/Basol	Sites	Vacuumless CIS

7/05/95	IEC/Meyers	Granata	CdTe Team Project
7/10/95	IEC/Meyers	Schmidt	CdTe Bias Stress
7/18/95	ISET/Basol	Sharp	Kapton Cells
9/05/95	Siemens/Tarrant	Granata	CIS Measurements
10/09/95	NREL/Albin	Granata	CdTe Measurements
10/11/95	Siemens/Tarrant	Granata	CIS Measurements
10/16/95	NREL/Albin	Granata	CdTe Measurements
11/30/95	Solarex/Kessler	Eisgruber	CIS Module Scans

REPORT DOCUMENTATION PAGE

Form Approved
OMB NO. 0704-0188

1. AGENCY USE ONLY (Leave blank)

2. REPORT DATE
August 1996

3. REPORT TYPE AND DATES COVERED
Annual Technical Report, 6 December 1994 - 5 December 1995

4. TITLE AND SUBTITLE
Device Physics of Thin-Film Polycrystalline Cells and Modules: Annual Subcontract Report, 6 December 1994 - 5 December 1995

5. FUNDING NUMBERS
C: XAX-4-14000-01
TA: PV631101

6. AUTHOR(S)
J.R. Sites

7. PERFORMING ORGANIZATION NAME(S) AND ADDRESS(ES)
Department of Physics
Colorado State University
Fort Collins, Colorado 80523

8. PERFORMING ORGANIZATION REPORT NUMBER

9. SPONSORING/MONITORING AGENCY NAME(S) AND ADDRESS(ES)
National Renewable Energy Laboratory
1617 Cole Blvd.
Golden, CO 80401-3393

10. SPONSORING/MONITORING AGENCY REPORT NUMBER
TP-451-21586
DE96013077

11. SUPPLEMENTARY NOTES
NREL Technical Monitor: B. von Roedern

12a. DISTRIBUTION/AVAILABILITY STATEMENT

12b. DISTRIBUTION CODE
UC-1263

13. ABSTRACT *(Maximum 200 words)*

This report describes the work on a number of projects carried out at both the cell and the module level during the past year. We investigated the effects of CdS thickness in collaboration with six CdTe cell-fabrication laboratories; there appears to be a critical thickness, between 500 and 1000 Å depending on fabrication process, below which junction quality is degraded. Our experimental and modeling project showed that conduction-band offsets less than about 0.3 eV have little effect on the performance of a $CuInSe_2$ (CIS) or CdTe cell under the traditional assumption that the absorber material accounts for most of the depletion region. The work in several other cell projects included the role of Ga distribution in $Cu_{1-x}Ga_xSe_2$ (CIGS) cells, changes that occur in some cells over time, optical characterization of commonly used CdTe substrates and front contacts, and comparative characterization of CIGS cells where identical absorbers were combined with variations in window fabrication. Our work on the primary module-characterization project developed the successful use of chopping-frequency variation in a scanning beam to separate photocurrent and shunting problems affecting individual cells of an encapsulated module. Other module projects included modifications in analysis required by the typical module-cell geometry, the practical effect of nonuniformities in light intensity or cell temperature, and the advantages and pitfalls of forward bias across a module during a light scan.

14. SUBJECT TERMS
photovoltaics ; thin-film polycrystalline ; cells and modules

15. NUMBER OF PAGES
35

16. PRICE CODE

17. SECURITY CLASSIFICATION OF REPORT	18. SECURITY CLASSIFICATION OF THIS PAGE	19. SECURITY CLASSIFICATION OF ABSTRACT	20. LIMITATION OF ABSTRACT
Unclassified	Unclassified	Unclassified	UL